Near-infrared linewidth narrowing in plasmonic Fano-resonant metamaterials via tuning of multipole contributions

Wen Xiang Lim, [1, 2, 3] Song Han, [1, 2] Manoj Gupta, [1, 2] Kevin F. MacDonald, [3] Ranjan Singh[1, 2, *]

[1]Division of Physics and Applied Physics, School of Physical and Mathematical Sciences, Nanyang Technological University, Singapore 637371, Singapore
[2]Centre for Disruptive Photonic Technologies, The Photonics Institute, Nanyang Technological University, 50 Nanyang Avenue, Singapore 639798, Singapore
[3]Optoelectronics Research Centre and Centre for Photonic Metamaterials, University of Southampton, Southampton, SO17 1BJ, United Kingdom

Abstract

We report on an experimental and computational (multipole decomposition) study of Fano resonance modes in complementary near-IR plasmonic metamaterials. Resonance wavelengths and linewidths can be controlled by changing the symmetry of the unit cell so as to manipulate the balance among multipole contributions. In the present case, geometrically inverting one half of a four-slot (paired asymmetric double bar) unit cell design changes the relative magnitude of magnetic quadrupole and toroidal dipole contributions leading to enhanced quality factor, figure of merit and spectral tuning of the plasmonic Fano resonance.

*Email: ranjans@ntu.edu.sg

Metamaterials have been a subject of intense interest due to their ability to exhibit optical properties not commonly found in natural materials. By suitably engineering the size and geometry of metamaterials at the sub-wavelength scale, researchers have been able to exploit and manipulate electromagnetic waves to achieve various phenomena such as invisibility cloaking,[1-4] super lenses,[5-8] electromagnetically-induced transparency[9-11], and high quality-factor Fano resonances[12-15] offering a rich variety of applications in photonics and optics. Specifically, a Fano resonance is a scattering phenomenon resulting from destructive interference between a continuum background and a resonant mode, and is commonly recognized by its asymmetric lineshape. In 1935, Ugo Fano was the first to theoretically formulate an equation which adequately provides an explanation of this unique and distinct lineshape.[16] In the field of plasmonic metamaterials, various Fano resonant unit cell shapes and designs such as dolmen structures,[17-19] ring/disk nanocavities,[20-23] heptamers[24-28] and notably split ring resonators[29-33] have been explored in great detail. An uncomplicated design composed of paired asymmetric double bars (ADBs) has also been studied for its Fano resonance[34-39] and electromagnetically-induced transparency properties.[40-43] While computed charge distribution and field vectors are typically used as a visual mechanism to identify and attribute the origin of the Fano resonance in such structures, there has been little focus on quantitative and qualitative analysis of the role of the multipoles that contribute to the asymmetric line shape and the linewidth narrowing of Fano resonances in complementary nanostructures (paired asymmetric double slots in a thin plasmonic metal film). Complementary nanostructures are interesting due to the enhanced mode volume as a result of the tight confinement of the electromagnetic fields in the narrow empty spaces of the nanostructures (portions without metal). Since the mode volume is higher in these nanostructures, the interaction of the Fano cavity with any other dynamic material medium would be extremely strong. As such, multipole expansion analysis is applied to this simple design as an illustration of the way in which it can enrich the understanding of symmetry-broken metamaterials in complementary designs.

Here, we introduce a comparison between complementary nanostructures of paired ADBs in so-called "Fano" and "iFano" configurations (iFano denoting a 180˚ inversion of one ADB relative to the Fano geometry – as shown in Fig. 1), and report that in the iFano configuration, a larger figure of merit and quality factor can be achieved in the infrared regime as compared to the Fano configuration. Numerical simulations attribute the origin of a broad dipolar resonance to the electric dipole, and the asymmetric Fano lineshape is a consequence of the electric dipole interacting with the magnetic quadrupole and the toroidal dipole. Via a decomposition of the multipoles, we find that the magnetic quadrupole competes on the same scale as the toroidal dipole to narrow down the linewidth of the resonance. In addition, the iFano configuration offers large spectral tunability without the need to alter the periodicity or dimensions of the unit cell.

Fig. 1(a) illustrates a generic unit cell of the metamaterial nanostructure used in the present study, which comprises of four slots (two complementary ADBs) in a thin gold film. In the 'Fano' configuration the ADBs have the same orientation, while in the iFano configuration shown, one ADB is rotated by 180˚ with respect to the other. The period of the unit cell is fixed at p_x = 1400 nm and p_y = 700 nm, the long bar length is fixed at l = 420 nm, and the x-separation between ADBs within the unit cell is fixed at g = 80 nm. Within the double bars, the long and short bars are separated with a distance, d = 140 nm. The asymmetry of the nanostructures was controlled by varying the length of the short bar, s from 420 nm to 100 nm. The asymmetry parameter is defined as the ratio of the difference between the length of the long (l) and short (s) bars to the length of the long bar, $\boldsymbol{\alpha = \frac{l-s}{l}}$. Figs. 1(b-e) show SEM images of fabricated complementary (b, d) Fano and corresponding (c, e) iFano configurations for asymmetry parameters of 0.762 and 0.289 respectively. Experimental samples were fabricated in a 40 nm gold thin film evaporated onto a quartz substrate at a rate of 0.2 Å/s. Each array of complementary nanostructures has dimensions of 40 μm by 40 μm and is fabricated by focused-ion beam milling (FEI Helios Nanolab 650 DualBeam operating at 30 kV and 24 pA).

The reflectance spectra of fabricated nanostructures were measured using a microspectrophotometer (Jasco MSV-5200) with *y*-polarized incident light. Numerical simulations were carried out using commercial finite-difference time-domain Maxwell solver software (Lumerical FDTD) assuming plane wave illumination polarized in the *y*-direction. Periodic boundary conditions were imposed in the *x*- and *y*- directions; perfectly matched layers were set in the *z*-direction so that any incident waves do not reflect at the boundaries but are strongly absorbed. The optical constants of gold were taken from Johnson and Christy[44] and the refractive index of the quartz substrate was set to 1.5.

Figs. 2(a, b) show the reflectance spectra measured for *y*-polarized incident light propagating normal to the plane of the nanostructures. They clearly illustrate that in both configurations, the Fano resonance red-shifts with decreasing asymmetry accompanied by linewidth narrowing. For a pair of *symmetric* double bars in both configurations, the resonance broadens and resembles a simple dipole resonance at around 1300 nm. In contrast, for non-zero asymmetry parameters, the broad dipolar resonance evolves into a Fano resonance centred at around 1400 nm for the iFano configuration at the highest level of asymmetry (α = 0.762) - a wavelength that is shorter than the resonance wavelength of the Fano configuration at around 1600 nm. Numerically simulated reflectance spectra, shown in Figs. 2(c, d) are in excellent agreement with the experimentally observed optical response, with the slight discrepancies in resonance wavelengths being attributed to imperfections incurred during the fabrication process (i.e. deviations from the ideal rectilinear geometry assumed in modelling) and differences in the optical constants of materials used in the simulations. It is evident from Figs. 2(e, f) that for a given value of the asymmetry parameter, the linewidth of the iFano configuration is narrower than the Fano configuration. The blue-shift of the entire spectrum from the Fano to iFano configuration is a result of a decrease in the electromagnetic coupling between the in-plane modes of the long bars in the latter case.[45]

Quality factors of the plasmonic system were evaluated for both configurations at their respective resonances. Quality (Q) factor is a dimensionless parameter which determines the extent of radiative and non-radiative losses in the plasmonic resonator. It is calculated here as a ratio between the resonance wavelength, λ_0 and the full-width at half maximum, $\delta\lambda$ of the resonance dip in the reflectance spectra, $\boldsymbol{Q = \frac{\lambda_0}{\delta\lambda}}$. A plasmonic system is less damped when the Q-factor is higher, and the system can store more energy. As shown in Fig. 3, measured and simulated Q-factors for the Fano configuration increase with decreasing asymmetry to values of 34.9 and 45.7 respectively at α = 0.048. From simulations, the Q-factor of the iFano configuration reaches 75.4 at α = 0.048, a value more than 1.5 times (50%) larger than the corresponding Fano configuration. However, at these small values of the asymmetry parameter, experimental Q-factors cannot be evaluated due to the weakness of the resonance, which appears as a shoulder as opposed to a defined dip in the reflectance spectrum (Fig. 2(b)). Another parameter which characterises the overall performance of the Fano resonance is the figure of merit (FoM), defined as the product of the Q-factor and the peak-to-peak resonant intensity. The FoM parameter is crucial as it considers the trade-off between the quality factor and the intensity of the Fano resonance. Typically, the Q factor of a Fano resonant system decreases as the resonance intensity increases when the asymmetry in the system is increased. From Fig. 3, the measured and simulated FoM in both configurations suggest that the system has optimum performance near α = 0.4 and 0.3 respectively. We observe reasonable agreement between the measured and simulated trends in both the Q-factor and FoM of the Fano and iFano configurations.

To better understand the nature of the optical responses in different configurations and its influence on the linewidth narrowing, numerical calculations were performed using a multipole expansion of the electromagnetic fields. The calculated induced current densities in the nanostructures were used to compute the scattering power of several multipoles, which can be represented in the x, y, z Cartesian coordinate frame as follow[46-48]:

$$\textbf{Electric dipole moment}: \boldsymbol{P_\alpha = \frac{1}{i\omega}\int J_\alpha d^3 r},$$

$$\textbf{Magnetic dipole moment}: \boldsymbol{M_\alpha = \frac{1}{2c}\int (r \times J)_\alpha d^3 r},$$

$$\textbf{Toroidal dipole moment}: \boldsymbol{T_\alpha = \frac{1}{10c}\int [(r \cdot J) r_\alpha - 2r^2 J_\alpha] d^3 r},$$

$$\textbf{Electric quadrupole moment}: \boldsymbol{Q_{\alpha\beta} = \frac{1}{i2\omega}\int \left[r_\alpha J_\beta + r_\beta J_\alpha - \frac{2}{3}(r \cdot J)\delta_{\alpha\beta}\right] d^3 r},$$

$$\textbf{Magnetic quadrupole moment}: \boldsymbol{M_{\alpha\beta} = \frac{1}{3c}\int [(r \times J)_\alpha r_\beta + (r \times J)_\beta r_\alpha] d^3 r},$$

where c is the speed of light, J is the induced current density, and $\alpha, \beta = x, y$ and z.

In both configurations, this analysis reveals that the appearance of the broad resonance for paired symmetric double bars can be attributed to an electric dipole which oscillates in phase with incident electromagnetic waves. As the length of the short bar starts to decrease, the symmetry of the nanostructures is broken, resulting in the excitation of the Fano resonance. In the asymmetric case, crucial higher-order contributions come from the toroidal dipole and magnetic quadrupole alongside the fundamental electric dipole as illustrated in Fig. 4 (magnetic dipole and electric quadrupole contributions by comparison are negligible). In general, the electric dipole is highly radiative and couples easily with the driving field. Although the electric dipole plays a determinative role in the appearance of the Fano resonance, the higher-order contributions of the toroidal dipole and the magnetic quadrupole cannot be neglected. As the asymmetry between the double bars is introduced in both configurations, there is an increase in their contributions, and together they interact with the electric dipole to form an asymmetric Fano resonance. The consequence is the narrowing of the linewidth of the resonance wavelength and a higher *Q*-factor obtained as compared to the symmetric system.

A closer look at the total contributions of the scattering power by the major multipoles at resonance reveals that the sum of the scattering power due to the electric dipole, magnetic

quadrupole and toroidal dipole in the Fano configuration is greater than in the iFano configuration, as shown in Fig. 5(a). This accounts for the higher *Q*-factor observed for the iFano configuration as compared to the Fano configuration. To understand the individual roles of the toroidal dipole and magnetic quadrupole, we took a difference between their scattering powers and noticed that for all asymmetry, there is a larger difference in the iFano configuration as compared to the Fano configuration. In both configurations, as shown in Fig. 5(b), below an asymmetry parameter of $\alpha = 0.35$, the difference between the scattering powers of the toroidal dipole and magnetic quadrupole starts to diverge. This corresponds to the point at which the *Q*-factor in Fig. 3(b) increases more rapidly with decreasing asymmetry parameter in the iFano configuration as compared to the Fano-configuration. This indicates that the response of the magnetic quadrupole dominates the toroidal dipole in the iFano configuration. In the Fano configuration, the toroidal dipole slowly suppresses the response of the magnetic quadrupole and the difference starts to reduce. As a result, we can conclude that with regards to the linewidth narrowing of the Fano resonance, the magnetic quadrupole plays a significant role in the resonant line narrowing while the toroidal dipole competes with the magnetic quadrupole to broaden the resonance in complementary paired ADBs system. With the iFano configuration, we can increase the dominance of the magnetic quadrupole and narrow the linewidth to improve the *Q*-factor. Moreover, by simply inverting one ADB in the paired ADB unit cell, it is possible to blue-shift the near-infrared resonance by as much as 200 nm (~12.5%), providing for facile spectral tuning without change of structural dimensions.

In conclusion, multipolar decomposition provides an informative and broadly applicable approach to the analysis of resonant modes in complementary plasmonic metamaterial structures. For the complementary paired ADB metamaterial arrays presented in this work, such analysis demonstrates that the optical response of the nanostructures is mainly due to interactions between the electric dipole, magnetic quadrupole and the toroidal dipole. The plasmonic systems in ‘Fano’ and ‘iFano’ configurations (‘i’ denoting the geometric inversion

of part of the unit cell) are similar but for an iFano configuration, we could enhance the contribution of the magnetic quadrupole relative to the toroidal dipole which results in the linewidth narrowing of the Fano resonance. The achievable *Q*-factor in the iFano configuration is enhanced by as much as 1.5 times compared to the Fano-configuration. Aside from enhancing the *Q*-factor, it is notable here that the inverted configuration also provides a mechanism to widen the tunability in the infrared spectral range without a need to change the shape or dimensions of the metamaterial unit cell - a behaviour that may be of particular use in optical and bio-sensing applications.

Acknowledgements

This work is supported by research grants from Nanyang Technological University Start-up Grant No. M4081282, Singapore Ministry of Education Grant Nos. MOE2011-T3-1-005, and MOE2015-T2-2-103, and the Engineering and Physical Sciences Research Council, UK Grant No. EP/M009122/1.

Following a period of embargo, the data from this paper will be available from the University of Southampton research repository at http://doi.org/10.5258/SOTON/D0158.

References:

[1]D. Schurig, J. J. Mock, B. J. Justice, S. A. Cummer, J. B. Pendry, A. F. Starr, and D. R. Smith, Science **314**, 977 (2006).

[2]J. B. Pendry, D. Schurig, and D. R. Smith, Science **312**, 1780 (2006).

[3]H. Y. Chen, C. T. Chan, and P. Sheng, Nature Mater. **9**, 387 (2010).

[4]T. Ergin, N. Stenger, P. Brenner, J.B. Pendry, and M. Wegener, Science **328**, 337 (2010).

[5]N. Fang, H. Lee, C. Sun, and X. Zhang, Science **308**, 534 (2005).

[6]X. Zhang and Z. Liu, Nature Mater. **7**, 435 (2008).

[7]N. Fang, D. Xi, J. Xu, M. Ambati, W. Srituravanich, C. Sun, and X. Zhang, Nature Mater. **5**, 452 (2006).

[8]V. M. Shalaev, Nat. Photonics **1**, 41 (2007).

[9]S. Zhang, D. A. Genov, Y. Wang, M. Liu, and X. Zhang, Phys. Rev. Lett. **101**, 047401 (2008).

[10]J. Gu, R. Singh, X. Liu, X. Zhang, Y. Ma, S. Zhang, S. A. Maier, Z. Tian, A. K. Azad, H. T. Chen, A. J. Taylor, J. Han, and W. Zhang, Nat. Commun. **3**, 1151 (2012).

[11]N. Papasimakis, V. A. Fedotov, N. I. Zheludev, and S. L. Prosvirnin, Phys. Rev. Lett. **101**, 253903 (2008).

[12]B. Luk'yanchuk, N. I. Zheludev, S. A. Maier, N. J. Halas, P. Nordlander, H. Giessen, and C. T. Chong, Nat. Mater. **9**, 707 (2010).

[13]V. A. Fedotov, M. Rose, S. L. Prosvirnin, N. Papasimakis, and N. I. Zheludev, Phys. Rev. Lett. **99**, 147401 (2007).

[14]R. Singh, I. Al-Naib, W. Cao, C. Rockstuhl, M. Koch, and W. Zhang, IEEE Trans. Terahertz Sci. Technol. **3**(6), 820 (2013).

[15]M. Rahmani, B. Luk'yanchuk, and M. Hong, Laser Photonics Rev. **7**, 329 (2013).

[16]U. Fano, Phys. Rev. **124**, 1866 (1961).

[17]N. Verellen, Y. Sonnefraud, H. Sobhani, F. Hao, V. V. Moshchalkov, P. V. Dorpe, P. Nordlander, and S. A. Maier, Nano Lett. **9**, 1663 (2009).

[18]B. Gallinet and O. J. F. Martin, Phys. Rev. B **83**, 235427 (2011).

[19]Y. Francescato, V. Giannini, and S. A. Maier, ACS Nano **6**, 1830 (2012).

[20]Y. Sonnefraud, N. Verellen, H. Sobhani, G. A. E. Vandenbosch, V. V. Moshchalkov, P. Van Dorpe, P. Nordlander, and S. A. Maier, ACS Nano **4**, 1664 (2010).

[21]Y. H. Fu, J. B. Zhang, Y. F. Yu, and B. Luk'yanchuk, ACS Nano **6**, 5130 (2012).

[22]A. E. Cetin and H. Altug, ACS Nano **6**, 9989 (2012).

[23]Y. Zhang, T. Q. Jia, H. M. Zhang, and Z. Z. Xu, Opt. Lett. **37**, 4919–4921 (2012).

[24]J. B. Lassiter, H. Sobhani, J. A. Fan, J. Kundu, F. Capasso, P. Nordlander, and N. J. Halas, Nano Lett. **10**, 3184 (2010).

[25]N. A. Mirin, K. Bao, and P. Nordlander, J. Phys. Chem. A **113**, 4028 (2009).

[26]M. Hentschel, M. Saliba, R. Vogelgesang, H. Giessen, A. P. Alivisatos, and N. Liu, Nano Lett. **10**, 2721 (2010).

[27]J. A. Fan, C. Wu, K. Bao, J. Bao, R. Bardhan, N. J. Halas, V. N. Manoharan, P. Nordlander, G. Shvets, and F. Capasso, Science **328**, 1135 (2010).

[28]A. E. Miroshnichenko and Y. S. Kivshar, Nano Lett. **12**, 6459–6463 (2012).

[29]K. Aydin, I. Bulu, K. Guven, M. Kafesaki, C. M. Soukoulis, and E. Ozbay, New J. Phys. **7**, 168 (2005).

[30]R. Singh, I. A. Al-Naib, Y. Yang, D. R. Chowdhury, W. Cao, C. Rockstuhl, T. Ozaki, R. Morandotti, and W. Zhang, Appl. Phys. Lett. **99**, 201107 (2011).

[31]Y. H. Fu, A. Q. Liu, W. M. Zhu, X. M. Zhang, D. P. Tsai, J. B. Zhang, T. Mei, J. F. Tao, H. C. Guo, X. H. Zhang, J. H. Teng, N. I. Zheludev, G. Q. Lo, and D. L. Kwong, Adv. Funct. Mater. **21**, 3589 (2011).

[32]R. Singh, I. A. Al-Naib, M. Koch, and W. Zhang, Opt. Express **19**, 6312 (2011).

[33]I. Al-Naib, R. Singh, C. Rockstuhl, F. Lederer, S. Delprat, D. Rocheleau, M. Chaker, T. Ozaki, and R. Morandotti, Appl. Phys. Lett. **101**(7), 071108 (2012).

[34]Y. Moritake, Y. Kanamori, and K. Hane, Opt. Lett. **39**, 4057 (2014).

[35]Y. Moritake, Y. Kanamori, and K. Hane, Appl. Phys. Lett. **107**, 211108 (2015).

[36]Y. Moritake, Y. Kanamori, and K. Hane, Opt. Express, **24**, 9332 (2016).

[37]D. J. Cho, F. Wang, X. Zhang, and Y. Ron Shen, Phys. Rev. B **78**, 121101 (2008).

[38]J. Wang, X. Liu, L. Li, J. He, C. Fan, Y. Tian, P. Ding, D. Chen, Q. Xue, and E. Liang, J. Opt. 15, 105003 (2013).

[39]F. Zhang, X. Huang, Q. Zhao, L. Chen, Y. Wang, L. Qiang, X. He, C. Li, and K. Chen, Appl. Phys. Lett. **105**, 172901 (2014).

[40]N. Niakan, M. Askari, and A. Zakery, J. Opt. Soc. Am. B **29**, 2329 (2012).

[41]X. R. Jin, J. Park, H. Zheng, S. Lee, Y. Lee, J. Y. Rhee, K. W. Kim, H. S. Cheong, and W. H. Jang, Opt. Express **19**, 21652 (2011).

[42]Z.-G. Dong, H. Liu, M.-X. Xu, T. Li, S.-M. Wang, S.-N. Zhu, and X. Zhang, Opt. Express **18**, 18229 (2010).

[43]N. E. J. Omaghali, V. Tkachenko, A. Andreone, and G. Abbate, Sensors **14**, 272 (2014).

[44]P. B. Johnson and R. W. Christy, Phys. Rev. B **6**, 4370 (1972).

[45]E. Prodan, C. Radloff, N. J. Halas, and P. Nordlander, Science **302**, 419 (2003).

[46]E.E. Radescu and G. Vaman, Phys. Rev. E **65**, 046609 (2002).

[47]T. Kaelberer, V. A. Fedotov, N. Papasimakis, D. P. Tsai, and N. I. Zheludev, Science 330, 1510 (2010).

[48]V. A. Fedotov, A. V. Rogacheva, V. Savinov, D. P. Tsai, and N. I. Zheludev, Sci. Rep. 3, 2967 (2013).

Figures and Figure Captions

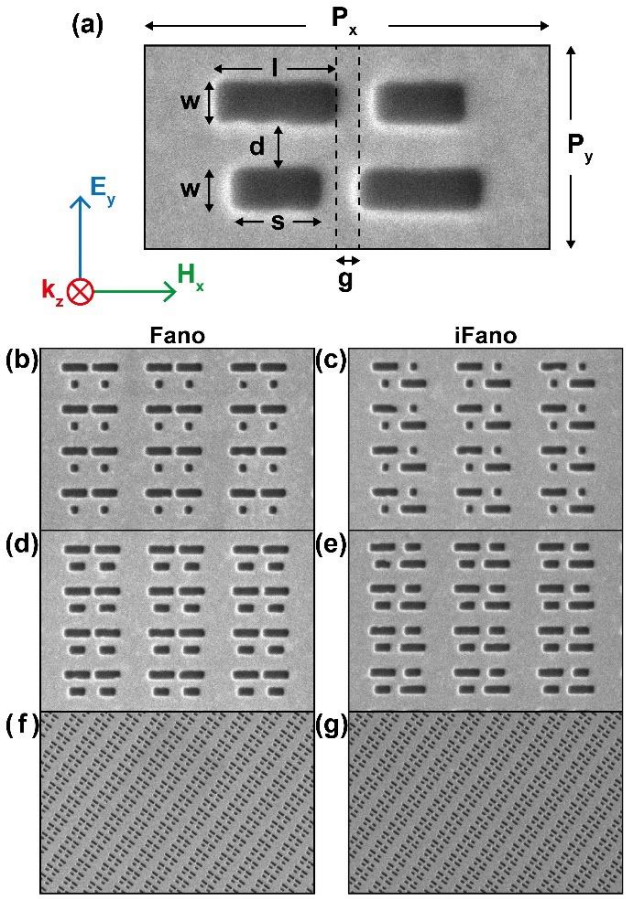

Figure 1. (a) Dimensions of a single unit cell of paired ADBs in the iFano configuration. The light is normally incident to the plane of the nanostructure with the electric field polarized along the *y*-axis and magnetic field in the *x*-axis. Scanning electron microscope (SEM) images of the complementary Fano nanostructures in the **(b, d)** Fano and **(c, e)** iFano configurations corresponding to asymmetry parameters of 0.762 and 0.286. Perspective view of **(f)** Fano and **(g)** iFano configurations at a tilted angle of 52˚.

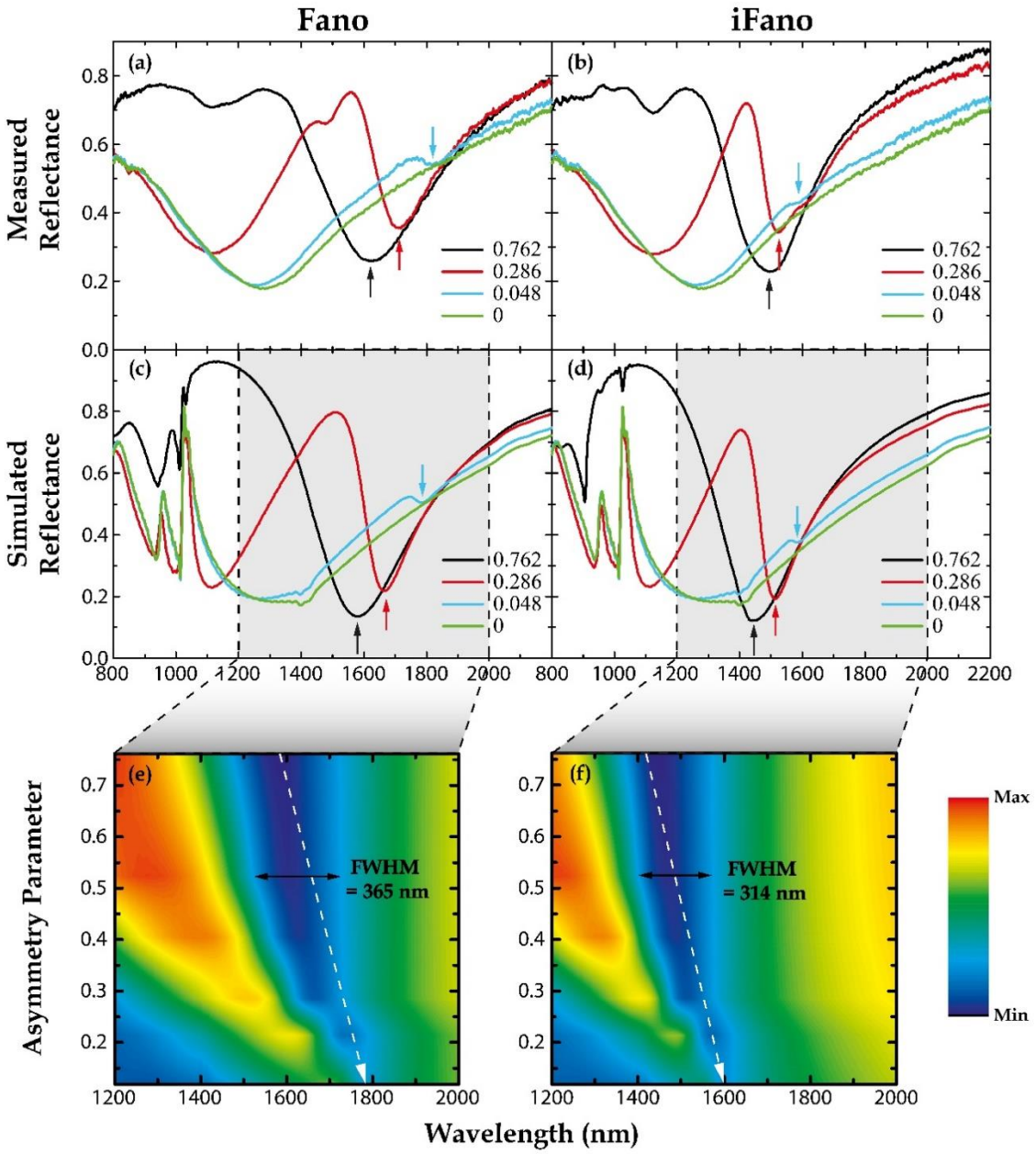

Figure 2. Measured and simulated reflectance spectra of the complementary **(a, c)** Fano and **(b, d)** iFano configurations at different asymmetry parameters. The dip of the Fano resonances are marked with coloured solid arrows corresponding to their asymmetry parameters in the reflectance spectra. Intensity plots of the **(e)** Fano and **(f)** iFano configuration at different asymmetries. In these figures, the black double arrow line depicts linewidth of the Fano resonance for $\alpha = 0.524$. The white line illustrates the tunability of the spectral range with different asymmetry parameters.

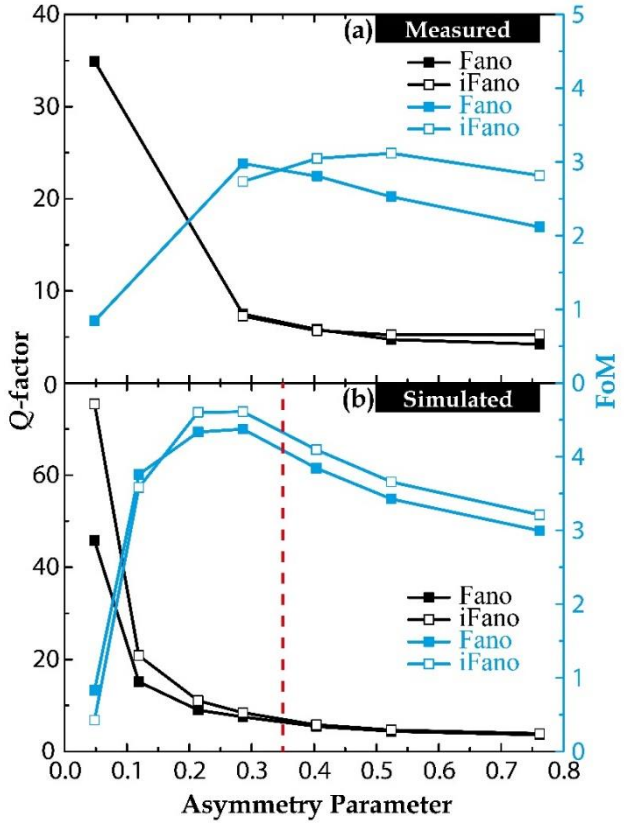

Figure 3. (a) Measured and **(b)** simulated *Q*-factor and FoM of the complementary Fano and iFano configurations for different asymmetry parameters.

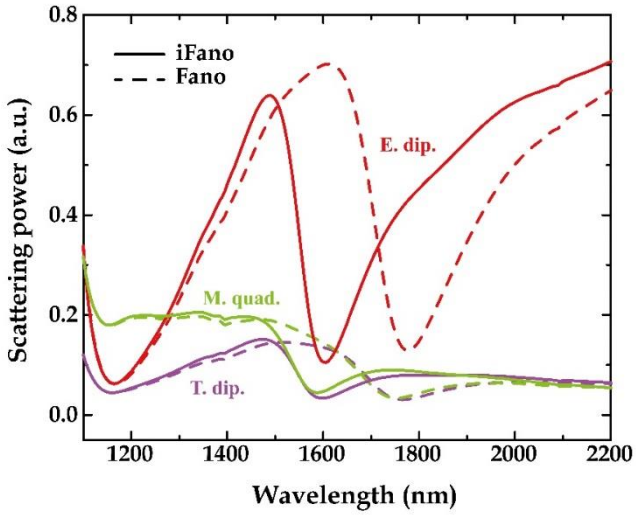

Figure 4. The scattering power of the major multipoles evaluated from the induced current densities of a unit cell in Fano (dotted lines) and iFano (solid lines) configurations for an asymmetry parameter of 0.289. Electric dipole (E. dip.) contributes the largest to the lineshape of the resonance. There are almost equal contributions to the scattering power from the

magnetic quadrupole (M. quad.) and toroidal dipole (T. dip.) at the resonance dip for both Fano and iFano configurations. Not shown in this figure are magnetic dipole and electric quadrupole, due to their negligible contributions.

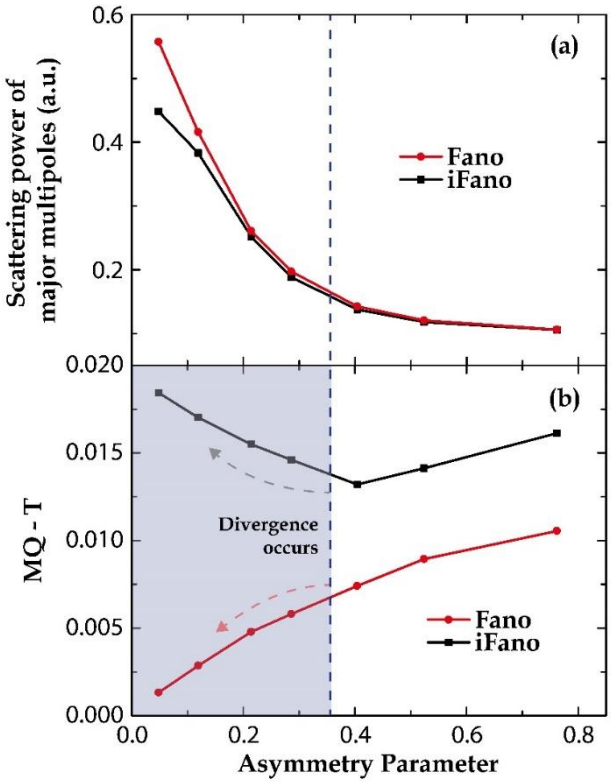

Figure 5. (a) The sum of the major multipoles evaluated from the induced current densities of a unit cell in the metamaterial at the Fano resonance. The Fano configuration has a higher scattering power than the iFano configuration. **(b)** The difference in the scattering power between magnetic quadrupole (MQ) and the toroidal dipole (T) is evaluated at the dip of the Fano resonance for both configurations.